Analytical Methods

RSC Publishing

PAPER

Method for measurement of friction forces on single cells in microfluidic devices

Cite this: *Anal. Methods*, 2012, 4, 4303

Lazar Milovanovic[a] and Hongshen Ma*[bcd]

We present a technique for measuring the static and kinetic friction forces between single cells and engineered surfaces in microfluidic channels. Frictional forces are defined as the sum of the non-specific attractive forces between two surfaces in sliding contact. The microchannels are fabricated using polydimethylsiloxane (PDMS) and modified using polyethylene glycol (PEG). Rectangular microchannels are designed to apply a modest compression (10–30%) to individual cells along one axis. Infusing a cell suspension into this channel at a precisely controlled flow rate enables the application of piconewtons of hydrodynamic drag force to each cell. At certain flow rates, the sample cells are separated into a population trapped by friction and a population where the hydrodynamic drag force overcomes friction. The kinetic friction force is measured as a function of cell compression using the velocity difference between free-flowing cells and the fluid. The upper bound static friction force is measured as a function of cell compression by analyzing the size distributions of trapped and free-flowing cells. Specifically, in order to overcome the coupled uncertainties associated with the normal force and the coefficient of friction, the upper bound static friction is estimated using the frictional force overcome by the largest free-flowing cell in the sampled population. Finally, the friction–reduction property of PEGylated surfaces is evaluated using the ratio of trapped *versus* free-flowing cells. The kinetic friction force between LCC6/Her2 cells and PEGylated PDMS was measured to range from 45 to 370 pN for cells under compression from 10% to 30%. Similarly, the upper bound static friction forces were measured to range from 50 to 700 pN for the same compression range.

Received 12th July 2012
Accepted 17th October 2012

DOI: 10.1039/c2ay25740h

www.rsc.org/methods

Introduction

Friction between biological cells and engineered surfaces is important for microfluidic devices designed to process cellular samples,[1,2] as well as surface coatings designed to reduce inflammation caused by implanted devices.[3–6] In the former case, frictional interactions can cause undesired cell trapping, which may result in blockages in microchannels. A quantitative estimate of friction would enable designers to determine the minimum flow rate necessary to avoid undesired cell trapping to ensure reliable device operation. Additionally, in the studies of cell biomechanics,[7–9] such estimates would enable frictional properties to be uncoupled from other biomechanical properties, such as cell deformability. For implanted devices, quantitative measurement of single cell friction could be used to evaluate the quality of surface coatings in order to improve patient comfort and reduce inflammation.[10–13]

Friction is defined as the force resisting the relative motion between two surfaces in sliding contact. The origin of this force is generally considered to be a combination of microscopic surface roughness and non-specific chemical adhesion.[14] Previous research on cell adhesion has sometimes used the term 'friction' to describe the adhesive force between biological cells and artificial surfaces.[15] In this paper, we specifically define friction as the force resisting relative motion in the presence of a normal force between the cell and the surface.

Techniques for measuring friction between macroscopic surfaces, under both dry and wet conditions, are well established.[16,17] The measurement of friction at micrometer and smaller length scales is more challenging. Recent studies have used a variety of techniques to measure the friction between dry microscopic surfaces, including atomic force microscopy, friction-force microscopy, surface-force apparatus, and quartz-crystal microbalance.[18–20] Methods to measure friction between microscopic wet surfaces, especially on cellular surfaces, are currently not available. Methods that have been developed for measuring dry friction cannot be directly adapted for wet friction measurements because they cannot easily uncouple viscous interactions from frictional interactions.

In this paper, we present a technique for measuring frictional forces between single cells and polydimethlysiloxane

[a]*Department of Physics and Astronomy, University of British Columbia, Canada*
[b]*Department of Mechanical Engineering, University of British Columbia, 2054-6250 Applied Science Lane, Vancouver, BC, Canada V6T 1Z4. E-mail: hongma@mech.ubc.ca*
[c]*Department of Urologic Science, University of British Columbia, Vancouver, BC, Canada*
[d]*Vancouver Prostate Centre, Vancouver General Hospital, Vancouver, BC, Canada*

(PDMS) microchannels. The surfaces of these microchannels are modified using polyethylene glycol (PEG), an industrial lubricant often used to reduce non-specific adhesion between artificial surfaces and biological materials.[21] We show that our technique is effective for estimating the magnitude of static and kinetic friction forces as a function of cell compression, as well as for evaluating the friction–reduction properties of surfaces modified using PEG.

Experimental approach

Our technique for measuring friction involves infusing single cells into a microfluidic channel that places these cells under slight compression as shown in Fig. 1. The height of the microfluidic channel is selected to compress each cell between 10% and 40% in order to generate appreciable normal force between the cell and the surface of the microchannel. Since PDMS is 3 orders of magnitude stiffer than typical biological cells, the deformation of PDMS is negligible relative to the deformation of each cell.[22] We restrict our test cells to phenotypes that are approximately spherical in shape and measure the amount of compression for each cell using the cross-sectional diameter of the cell in the transverse plane of the microchannel. LCC6/Her2 breast cancer cells were selected for our experiments because of their size, as well as the uniformity of their size distribution.

To measure the resistive force resulting from frictional interactions between the cell and the microchannel surface, a pressure difference applied across the channel is used to generate a precisely controlled flow of the bulk liquid. Friction forces acting on the cell impede their flow and the velocity difference relative to the bulk liquid can be used to determine the hydrodynamic force transferred to the cell. The Reynolds number of our experiment is $\sim 10^{-3}$, which means the hydrodynamic force transferred from the fluid to the cell can be estimated using a simple laminar flow model. This type of hydrodynamic force transfer has been used extensively to measure the adhesion force between single cells and artificial surfaces.[23,24]

To measure kinetic friction, we observed the movement of test cells while under compression in the microchannel. The difference between the flow rate of the cell and the flow rate of the bulk fluid can be used to determine the drag force transferred to the cell to overcome kinetic friction. In this case, a separate marker, such as a microparticle or a red blood cell, is used to determine the flow rate of the bulk fluid.

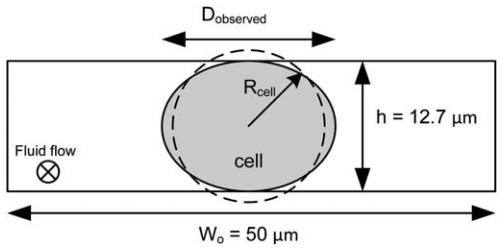

Fig. 1 Axial cross-section of a cell under compression in the microchannel. Fluid flow is into the page.

To measure static friction, we observed test cells near the critical point between free-flowing and being trapped by friction while under compression in the microchannel. As shown by the free-body diagram in Fig. 2, if the drag force, F_{Drag}, is less than the available static friction force, $F_{Fr,static}$, then the test cell remains stationary. If $F_{Drag} > F_{Fr,static}$, then the test cell will move with the fluid. Since the flow rate of the bulk liquid determines F_{Drag}, it is possible, in theory, to determine the critical F_{Drag} by repeating the experiment at various flow rates. In practice, however, this measurement is limited by several key challenges. First, friction is a highly stochastic process. Given identical materials and experimental conditions, the friction force experienced in each instance will show significant variation. Second, static friction is also hysteretic, which means that the friction measured from each cell depends on whether that the cell was previously moving or stationary. Finally, since every biological cell is unique, the parameters of each frictional interaction, including normal force and the coefficient of friction, are coupled and cannot be applied repeatedly for the purpose of ensemble averaging.

We overcome these challenges by infusing a small population of cells into a constrained microchannel at a flow rate where we expect a portion of these cells to be free-flowing and a portion to be trapped by friction. If the friction force is entirely deterministic, then we expect the cell sample to be divided at a critical compression ratio with minimal overlap between the free-flowing and trapped cells as shown in Fig. 3. However, because of the stochastic nature of friction and the differences

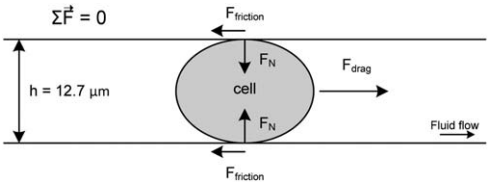

Fig. 2 Free-body diagram of a cell constrained in a microchannel.

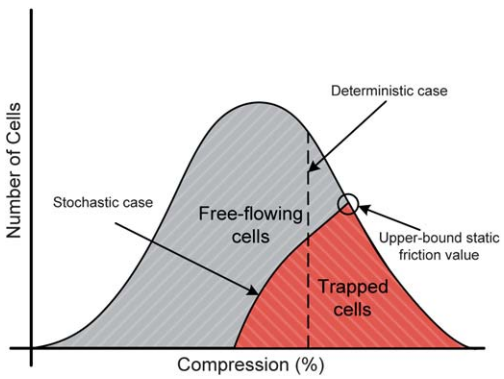

Fig. 3 The expected distribution as a function of compression when a population of cells is constrained in a microchannel. If friction is entirely deterministic, then a sharp transition between moving and free-flowing cells is expected. Accounting for the stochastic nature of friction, the trapped and free-flowing cell populations are expected to overlap as shown.

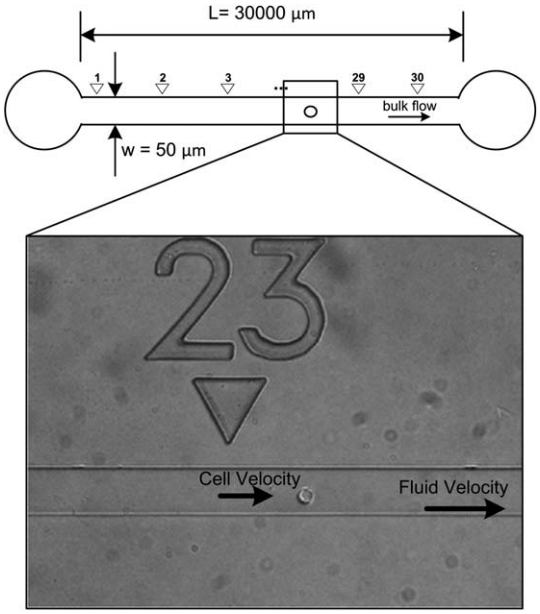

Fig. 4 Diagram of the microfluidic device used in experiments. Inset shows a single cell being tracked as it traverses the microfluidic channel near a fiducial marking to measure cell velocity on a moving microscopic stage.

between cells, the distributions of free-flowing and trapped cells are expected to overlap as shown in Fig. 3. Therefore, we can estimate the upper bound value of the static friction force using the drag force experienced by the free-flowing cell that experiences the greatest compression in a test cell population. This approach produces a robust estimation of the upper bound of the friction force because the compressive force experienced by the cell increases sharply with the compression ratio. Consequently, the probability of finding a free-flowing cell is dramatically reduced for cells compressed beyond the critical compression as found in the deterministic case.

The microfluidic device used in this study is a long rectangular PDMS microchannel that is 12.7 μm × 50 μm in cross-section and 30 mm in length (Fig. 4). The microchannel is augmented with fiducial markers every 1000 μm in order to facilitate cell velocity measurement on a moving microscope stage. LCC6/Her2 breast cancer cells have a mean diameter of 14.3 ± 1.33 μm, which means a significant fraction of these cells will be under compression between 10% and 35% in the 12.7 μm channel.

Materials and methods

Photolithographic microfabrication

A mask for microfabrication was designed using SolidWorks DWG Editor and manufactured by Advance Reproductions (North Andover, MA, USA). A mold of the desired microstructures was fabricated on silicon wafers using SU-8 3005 photoresist (MicroChem, Newton, MA, USA) on a 100 mm diameter silicon wafer. The wafer is first cleaned using solvents and then dehydration baked on a hotplate at 200 °C for 5 min. Next, SU-8 3010 was spread onto the wafer at 1500 rpm for 30 s. The wafer was then soft baked at 95 °C on a hotplate for 7 min before being exposed to UV light in a mask aligner for 30 s. The exposed wafer was given a post-exposure bake in the sequence of 65 °C for 1 min, 95 °C for 1.5 min and then 65 °C for 1 min. The wafer was then developed using SU-8 developer (Micro-Chem). The geometry of the SU-8 photoresist was stabilized by further baking on a hotplate at 200 °C for 1 hour.

Soft-lithography of PDMS

Replicas of the microstructures fabricated on the silicon wafer were fabricated using a polyurethane-based plastic (Smooth-Cast 310, Smooth-On, Easton, PA, USA) using the process described by Desai *et al.*[25] These plastic molds were used to fabricate the microfluidic devices using soft-lithography of PDMS. Sylgard-184 PDMS (Momentive Performance Materials, Columbus, OH, USA) was poured onto the microchannel mold at a ratio of 10 : 1 base to hardener. The mold with pre-cured PDMS was then degassed in a vacuum desiccator for 15 min and then baked in an oven for 240 min at 65 °C. After cooling, the device was removed from its mold, and holes were punched into it using a 0.5 mm diameter hole punch (Technical Innovations, Angleton, TX, USA) as the fluidic inlet and outlet ports. A standard glass microscope slide (Fisher Scientific) was cleaned using acetone and then thoroughly rinsed with de-ionized H_2O. The microfluidic channel is assembled by bonding the PDMS structure with the microscope slide after exposure to air plasma (Model PDC-001, Harrick Plasma, Ithaca, NY, USA) for 40 s.

Cell sample preparation

The LCC6/Her2 cells were cultured using standard *in vitro* conditions as adherent monolayer cultures in 25 cm^2 Falcon flasks in DMEM (Gibco-Invitrogen) supplemented with 10% fetal bovine serum (Invitrogen) and 1% penicillin/streptomycin (Invitrogen). The cells were incubated at 37 °C with 100% humidity and 5% CO_2. The cell samples used in experiments were LCC6/Her2 cells suspended in DMEM medium. Fixed red blood cells were added at the concentration of 5% (by volume), along with 7.5% bovine serum albumin (Invitrogen). Fixed red blood cells used as markers to measure flow velocities were obtained from reagent kits used for immunotyping (Medion Diagnostics, Miami, FL, USA).

Surface PEGylation

PDMS surfaces were modified with covalent bonding of PEG using polyethylene-glycol-methyl-ether-methacrylate (PEG-MEM) (Sigma-Aldrich), following the procedure outlined by Zhou *et al.* where PEGMEM is mixed with PDMS before curing.[26] PEGMEM-modified PDMS devices were tested and compared with a control PDMS device for cell build-up and surface adhesion. Covalently bonded PEGMEM was tested in 0.5, 0.75, 1.0 and 1.5% by weight in the PDMS device.

Experimental apparatus

15 ml falcon tubes (Fisher Scientific) containing samples and buffer fluids were sealed with custom-designed caps acting as pressurized reservoirs to feed fluids into the microchannel.

Liquid connections between falcon tubes and the PDMS microfluidic device were made using 0.5 mm ID flexible Tygon tubing (Cole-Parmer). The Tygon tubing and the PDMS device were interfaced using 19 mm long 23-gauge stainless steel tubing (New England Small Tube, Litchfield, NH, USA) that formed an elastic, watertight seal on both ends. The PDMS devices was mounted and secured to the moving microscope stage prior to experiment.

Data collection

The motion of single cells inside the microfluidic channel was tracked using a Nikon Ti-U inverted microscope with a Nikon DS-2MBWc camera and Nikon NIS-Elements software. Cell diameters were measured using a 10× objective and the spherical diameter measurement tool included in the Nikon NIS-Elements software. Precisely controlled pressure applied across the microfluidic channel was produced using a Fluigent MFCS-4C pressure controller (Paris, France). In the studies of kinetic friction, fixed red blood cells were used to measure the flow rate of the bulk fluid.

Finite element model of the fluid drag force

A finite element model was created using the Microfluidics Module in COMSOL Multiphysics (Los Angeles, CA, USA) to determine the fluid drag force experienced by each cell. Each cell was modeled as a neutrally buoyant, symmetric ellipsoid at the center of a long microchannel. The length of the device was reduced from 30 000 μm to 3000 μm in order to reduce meshing complexity. Since the hydrodynamic resistance of a rectangular channel decreases linearly with the decrease in length, the applied pressure difference is also scaled proportionately. We simulated the flow field around the cell and determined the fluid drag force by integrating the flow field along the cell boundary.

The model was meshed as two separate regions in order to reduce the computation time. A cylindrical area of 20 μm diameter around the ellipsoid was meshed with a free triangular mesh. The remainder of the channel, not used for the flow profile measurement, was meshed with a free triangular mesh with no defined maximum element size. This simulation was performed for each measured cell diameter and flow rate reported in the Results and discussion section to determine the drag force applied to each cell.

Results and discussion

Using surface PEGylation to reduce friction

We investigated the use of surface PEGylation to reduce the non-specific adhesion of cells in microchannels by infusing a cell sample into the constrained microchannel at a fixed flow rate. The microchannels had a thickness of 12.7 μm and were modified using 0.5%, 1.0%, and 1.5% polyethylene glycol methyl ether methacrylate (PEGMEM). A constant pressure difference was used to generate a flow rate of 570 μm s^{-1} ± 50 μm s^{-1}, which was measured by tracking the flow of fixed red-blood cells.

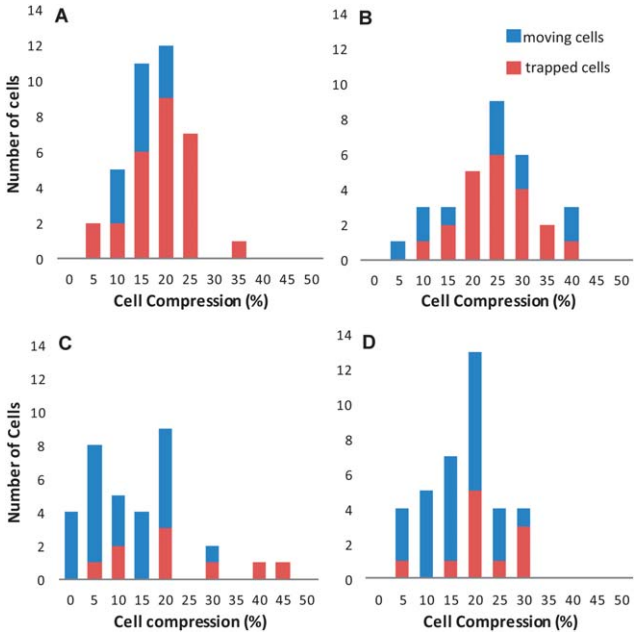

Fig. 5 Distribution of trapped and free-flowing cells in a single (A) untreated PDMS microchannel, and PDMS microchannels PEGylated using (B) 0.5%, (C) 1.0%, and (D) 1.5% PEGMEM. Trapped cells are shown in red, while free-flowing cells are shown in blue.

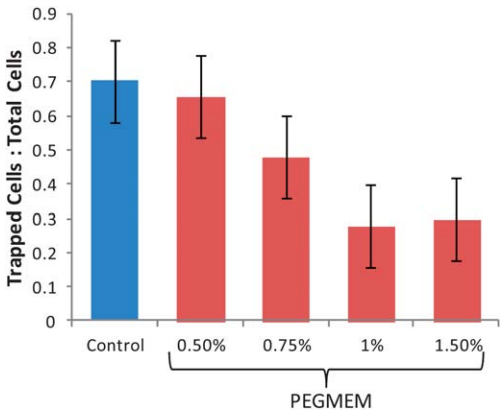

Fig. 6 Comparison of the ratio of trapped cells to total cells in a microchannel treated with varying amounts of PEGMEM.

The population of trapped and free-flowing cells in the control and PEGylated PDMS microchannels is shown in Fig. 5 as a function of cell compression. These data graphs show a distribution of trapped and free-flowing cells as predicted in Fig. 3. The number of trapped cells appears to decrease significantly with increasing PEGMEM concentration. The ratio of trapped cells to the total number of cells is summarized in Fig. 6. The fraction of trapped cells is reduced by one-half from control microchannels to microchannels PEGylated with 1.0% PEGMEM. There appears to be no difference in the ratio of trapped cells between the 1.0% and 1.5% PEGMEM microchannels, which suggests that there is no additional benefit derived from adding more than 1% PEGMEM to the PDMS

material. This observation is noteworthy because the PEGMEM additive reduces the optical transparency of PDMS, which is important for many biological experiments.

Measurement of static friction

We estimated the upper bound value of the static friction force between single cells and PDMS microchannel surfaces using the flow properties of LCC6/Her2 cells constrained in microchannels PEGylated using 1.5% PEGMEM. Similar to the previous experiment, we infused ~50 cells under slight compression into a 12.7 μm microchannel using a precisely controlled flow rate. For a fraction of these cells, the applied drag force is insufficient to overcome the resistance provided by the static friction force, and as a result, the cells are trapped in the channel. For the complementary fraction, the applied drag force is sufficient to overcome the static friction force, and the cells slide along the channel with the fluid. In this case, larger moving cells must overcome greater friction force because these cells experience greater compressive forces. Therefore, the hydrodynamic force experienced by the largest moving cell provides an effective estimate of the upper bound static friction force.

We obtained the distributions of trapped and free-flowing cells at several flow rates in order to apply different ranges of drag forces to the cell population. These results are shown as a function of cell compression ratio in Fig. 7. The flow rate of the bulk liquid was selected to cover the range of trapped *versus* free-flow cell populations. The lower end of this range (Fig. 7A) was selected such that multiple free-flowing cells could be found in the microchannel. The upper end of this range (Fig. 7E) is limited by the frame rate of the video camera used to track the position of the cells in order to measure their flow rate. The data shown in Fig. 7 only include cells under compression. A few smaller, uncompressed cells travelling through the device were observed but not recorded. The number of cells measured in each experiment varies because the rate of entry of cells into the microchannel is proportional to the pressure difference across the device. The mean diameter of the cell population decreased with decreasing fluid flow rates because larger cells could be pushed into the microchannel at greater flow rates. The compression ratio where the largest moving cell is found was generally unambiguous. However, a single outlier was observed in one of the experiments, where a single moving cell was found to be significantly larger than any other trapped cell in the channel (Fig. 7D). This cell appeared to have a greater cytosol volume compared to other cells, but did not have an abnormal shape or other visible abnormal characteristics by which it could be excluded from the experimental dataset. This cell was the only instance where a moving cell was found to be larger than the largest trapped cell in the microchannel.

For each of the largest moving cells in Fig. 7, we estimate the uncompressed cell diameter by measuring the diameter of the cell in the transverse plane of the microchannel and assuming that the cell compresses to an ellipsoidal shape with conserved volume. The radius of the uncompressed cell is therefore,

$$R_{\text{cell}} = \left(\left(\frac{h}{2}\right) R_{\text{transverse}}{}^{2}\right)^{\frac{1}{3}}$$

where h is the height of the microchannel, which is set at 12.7 μm. Modeling each cell as a symmetric ellipsoid located at the center of a rectangular channel, we used a finite element model (COMSOL Multiphysics) to calculate the hydrodynamic drag force by integration of the fluid flow field on the surface of each cell. In reality, the deformed cell is likely to take a shape

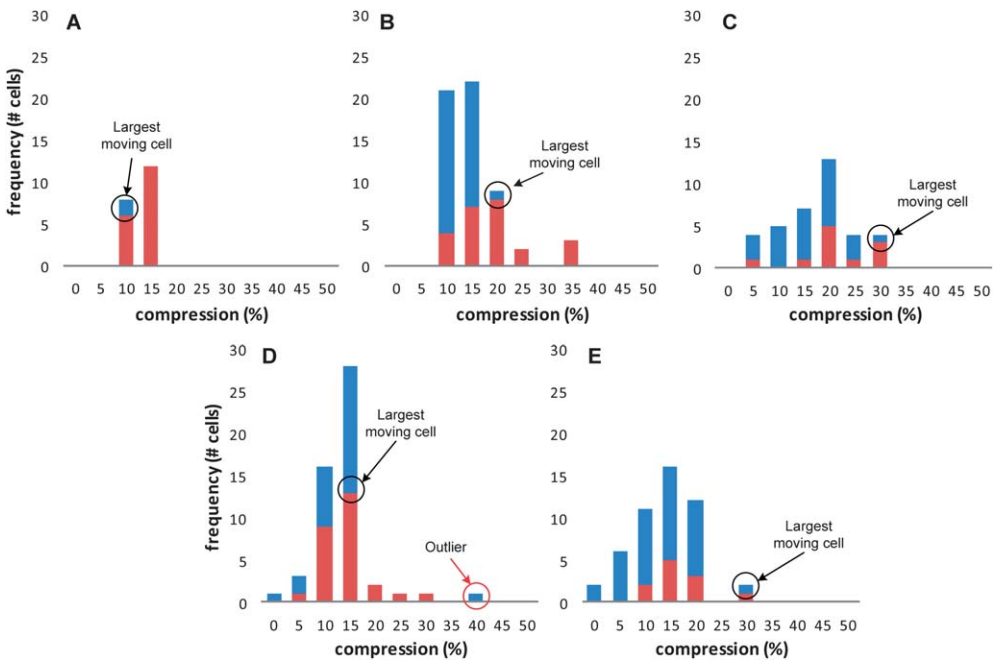

Fig. 7 Distributions of trapped and free-flowing cells. Distributions were obtained at flow rates of (A) 195, (B) 401, (C) 654, (D) 711, and (E) 853 μm s^{-1}. The largest moving cell is identified in each case. A single outlier was observed in subplot D.

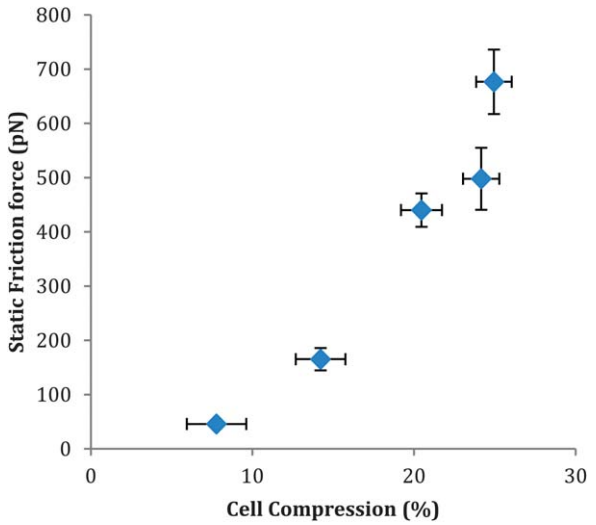

Fig. 8 Upper bound static friction force as a function of cell compression determined from each dataset shown in Fig. 7.

that is an intermediate between an ellipsoid and a sphere with flattened ends. For the purpose of hydrodynamic modeling, however, this difference in shape is negligible and the ellipsoidal shape provides a consistent method to estimate the radius of the uncompressed cell.

The upper bound static friction, obtained from the largest moving cell in each subplot in Fig. 7, is shown as a function of cell compression in Fig. 8. The upper bound static friction force was measured to range from 50 to 700 pN for cells compressed from 10% to 30%. An average sized LCC6/Her2 cell, 15 μm in diameter and compressed to 15% by the 12.7 μm microchannel, is expected to experience an upper bound static friction force of approximately 200 pN. The shape of the data graph suggests a linear or an exponential relationship; however, measurement over a greater cell compression range is required to further quantify this relationship. The experimental uncertainty of the data shown in Fig. 8 derives from the measurement of the cell diameter and the flow rate of the fluid. The former is limited by the optics of the microscope and camera resolution. While the latter is limited by the uncertainty in the velocity of fixed red blood cells that are used to determine the flow rate of the fluid.

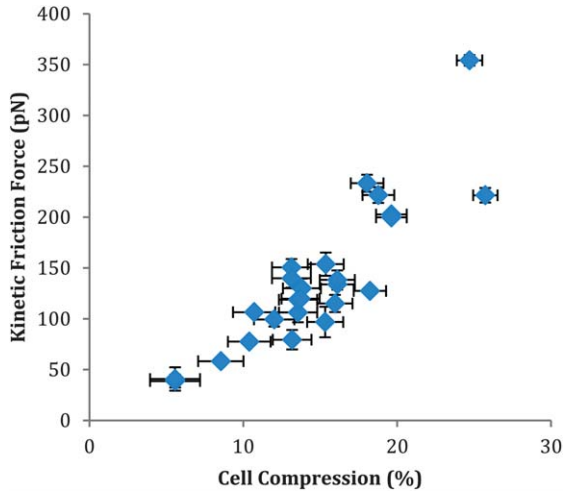

Fig. 9 Kinetic friction as a function of cell compression. Results were collected from multiple experiments performed using different devices.

Measurement of kinetic friction

To measure the kinetic friction experienced by single cells, we tracked cells moving at an approximately constant velocity while constrained in PDMS–glass microchannels where the PDMS part has been treated with 1.5% PEGMEM. Similar to previous experiments, we infused approximately 50 cells into the microfluidic device. The compressed diameter of these cells was measured as before. Fixed red blood cells were added to the cell mixture to measure the speed of the fluid to determine the drag force applied to each cell. To minimize channel edge effects that may reduce the drag force experienced by the cell, we selected cells that were moving in the center of the microchannel and excluded cells near the edge of the microchannel. We also excluded non-spherical cells from our measurement similar to the static friction measurement.

The drag force applied to each cell by the carrier fluid is proportional to the relative velocity between the cell and the fluid. From the measured cell size and relative velocity, we again used our finite element model of an ellipsoid centered in a microchannel to determine the drag force on a cell as in the static friction case. The kinetic friction data are shown in Fig. 9. Expectedly, the measured kinetic friction increases with increasing cell compression in the channel. The results shown in Fig. 9 were collected from multiple experiments performed using multiple microfluidic devices. The results were highly consistent. The kinetic friction force was measured to range from 45 to 370 pN for cells under compression from 10% to 30%. As expected, the measured kinetic friction was smaller than the static friction for the same cell compression range.

Conclusion

We developed a technique for measuring the static and kinetic friction forces between single cells and engineered surfaces in microfluidic channels. Using rectangular microchannels that apply a modest compression to single cells along one axis, cells infused into the microchannel at a precisely controlled flow rate separate into a population trapped by friction and a population where the hydrodynamic drag force overcomes friction. The friction–reduction property of PEGylated surfaces was determined using the ratio of trapped *versus* free-flowing cells. The upper bound static friction force was determined by analyzing the size distributions of trapped and free-flowing cells. The kinetic friction force was determined from the velocity difference between free-flowing cells and the fluid velocity. The static friction force between LCC6/Her2 cells and PDMS treated with 1.5% PEGMEM was measured to range from 50 to 700 pN for cells under compression from 10% to 30%. Under an identical compression range, the kinetic friction force was measured to range from 45 pN to 370 pN.

Acknowledgements

The authors would like to thank Jianxing Niu, Edison Lee, Lily So, and Sarah McFaul for technical assistance. The authors would like to thank Karen Cheung and Linfen Yu for providing materials used in this study. This work was supported by grants from the Bill and Melinda Gates Foundation, Natural Science and Engineering Research Council of Canada, and Canadian Institutes of Health Research.

References

1 B. Bhushan and Z. Burton, Adhesion and friction properties of polymers in microfluidic devices, *Nanotechnology*, 2005, **16**(4), 467–478.
2 S. M. McFaul, B. K. Lin and H. Ma, Cell separation based on size and deformability using microfluidic funnel ratchets, *Lab Chip*, 2012, **12**(13), 2369–2376.
3 D. T. Beiko, B. E. Knudsen and J. D. Denstedt, Reviews in endourology – advances in ureteral stent design, *J. Endourol.*, 2003, **17**(4), 195–199.
4 J. H. Kuiper and R. Huiskes, Friction and stem stiffness affect dynamic interface in total hip replacement, *J. Orthop. Res.*, 1996, **14**(1), 36–43.
5 H. Mckellop, I. Clarke, K. Markolf and H. Amstutz, Friction and wear properties of polymer, metal, and ceramic prosthetic joint materials evaluated on a multichannel screening device, *J. Biomed. Mater. Res.*, 1981, **15**(5), 619–653.
6 H. K. Mardis, R. M. Kroeger, J. J. Morton and J. M. Donovan, Comparative-evaluation of materials used for internal ureteral stents, *J. Endourol.*, 1993, **7**(2), 105–115.
7 B. K. Chen, Y. Zhang, D. D. Perovic and Y. Sun, MEMS microgrippers with thin gripping tips, *J. Micromech. Microeng.*, 2011, **21**(10), 105004.
8 Q. Guo, S. Park and H. Ma, Microfluidic micropipette aspiration for measuring the deformability of single cells, *Lab Chip*, 2012, **12**(15), 2687–2695.
9 M. Hagiwara, T. Kawahara, Y. Yamanishi and F. Arai, Driving method of microtool by horizontally arranged permanent magnets for single cell manipulation, *Appl. Phys. Lett.*, 2010, **97**(1), 013701.
10 G. Donelli, E. Guaglianone, R. Di Rosa, F. Fiocca and A. Basoli, Plastic biliary stent occlusion: factors involved and possible preventive approaches, *Clin. Med. Res.*, 2007, **5**(1), 53–60.
11 N. E. W. Hartley, Friction and wear of ion-implanted metals – review, *Thin Solid Films*, 1979, **64**(2), 177–190.
12 A. G. Mikos, L. V. McIntire, J. M. Anderson and J. E. Babensee, Host response to tissue engineered devices, *Adv. Drug Delivery Rev.*, 1998, **33**(1–2), 111–139.
13 U. Weickert, F. Wiesend, T. Subkowski, A. Eickhoff and G. Reiss, Optimizing biliary stent patency by coating with hydrophobin alone or hydrophobin and antibiotics or heparin: an *in vitro* proof of principle study, *Adv. Med. Sci.*, 2011, **56**(2), 138–144.
14 Z. Burton and B. Bhushan, Hydrophobicity, adhesion, and friction properties of nanopatterned polymers and scale dependence for micro- and nanoelectromechanical systems, *Nano Lett.*, 2005, **5**(8), 1607–1613.
15 D. A. Hammer and M. Tirrell, Biological adhesion at interfaces, *Annu. Rev. Mater. Sci.*, 1996, **26**, 651–691.
16 P. B. U. Andersson and W. Kropp, *Rapid Tyre/Road Separation: an Experimental Study of Adherence Forces and Noise Generation. Wear*, 2009. vol. 266(1–2), pp. 129–138.
17 B. N. J. Persson and A. I. Volokitin, Dynamical interactions in sliding friction, *Surf. Sci.*, 2000, **457**(3), 345–356.
18 B. Bhushan, J. N. Israelachvili and U. Landman, Nanotribology – friction, wear and lubrication at the atomic-scale, *Nature*, 1995, **374**(6523), 607–616.
19 J. Krim, D. H. Solina and R. Chiarello, Nanotribology of a Kr monolayer – a quartz-crystal microbalance study of atomic-scale friction, *Phys. Rev. Lett.*, 1991, **66**(2), 181–184.
20 Y. F. Mo, K. T. Turner and I. Szlufarska, Friction laws at the nanoscale, *Nature*, 2009, **457**(7233), 1116–1119.
21 *Poly(Ethylene Glycol): Chemistry and Biological Applications. ACS symposium series*, ed. J. M. Harris and S. Zalipsky, American Chemical Society, Washington, DC, 1997, p. 489.
22 G. Bao and S. Suresh, Cell and molecular mechanics of biological materials, *Nat. Mater.*, 2003, **2**(11), 715–725.
23 K. V. Christ, K. B. Williamson, K. S. Masters and K. T. Turner, Measurement of single-cell adhesion strength using a microfluidic assay, *Biomed. Microdevices*, 2010, **12**(3), 443–455.
24 H. Lu, L. Y. Koo, W. C. M. Wang, D. A. Lauffenburger, L. G. Griffith and K. F. Jensen, Microfluidic shear devices for quantitative analysis of cell adhesion, *Anal. Chem.*, 2004, **76**(18), 5257–5264.
25 S. P. Desai, D. M. Freeman and J. Voldman, Plastic masters-rigid templates for soft lithography, *Lab Chip*, 2009, **9**(11), 1631–1637.
26 J. H. Zhou, H. Yan, K. N. Ren, W. Dai and H. K. Wu, Convenient method for modifying poly(dimethylsiloxane) with poly(ethylene glycol) in microfluidics, *Anal. Chem.*, 2009, **81**(16), 6627–6632.